

# Construction and Humidity Response of a Room-Temperature-Phosphorescent Hybrid Xerogel Based on a Multicharge Supramolecular Assembly

Wen-Tao Fan, Yong Chen, Jie Niu, Ting Su, Jing-Jing Li, and Yu Liu\*

Organic room-temperature phosphorescence (RTP) has attracted tremendous attention in recent years due to its potential utility in combination with artificial soft materials. Herein, a room-temperature-phosphorescent hybrid xerogel held together by electrostatic and host–guest interactions is reported. The xerogel is constructed by noncovalent complexation of 7-[6-deoxy-6-(2-sulfonic)]- $\beta$ -cyclodextrin (SCD) with the phosphor bromophenyl-methyl-pyridinium chloride (PYCl) and in situ incorporation of the anionic SCD $\supset$ PYCl complex into a cationic amino clay (AC) via electrostatic interactions. The resulting xerogel, designated AC/SCD $\supset$ PYCl, has a network structure that can suppress vibrational and nonradiative relaxation of the phosphor, leading to green RTP emission as well as good fluorescence–phosphorescence dual emission. Notably, the intensity of the xerogel RTP varies with humidity and can be switched on and off repeatedly, which indicates that the xerogel has potential utility as an organic light-emitting humidity-sensing material.

## 1. Introduction

In recent years, organic materials with room-temperature phosphorescence (RTP) have attracted considerable research attention, mainly because of the wide variety of their applications, including as organic light-emitting diodes,<sup>[1]</sup> bioimaging agents,<sup>[2]</sup> photodynamic therapeutics,<sup>[3]</sup> and chemical sensors.<sup>[4]</sup> In particular, the combination of phosphorescent materials and artificial soft materials has recently become a research hotspot because such combinations have many potential applications, including as

stimulus-responsive materials,<sup>[5]</sup> optoelectronics,<sup>[6]</sup> and sensors,<sup>[7,8]</sup> due to their special optical and mechanical properties. However, spin coupling in pure organic molecules is weak, which makes the efficiency of intersystem crossing low and thus leads to weak phosphorescence.<sup>[9]</sup> Therefore, much effort has been devoted to developing new methods for achieving efficient RTP.


It has been widely studied that RTP materials can be constructed into supramolecular composites to enhance their phosphorescent behavior via host–guest interaction.<sup>[10]</sup> Various types of structures have been shown to facilitate intersystem transitions.<sup>[11]</sup> For example, phosphor crystallization or incorporation into inorganic clay can inhibit nonradiative transitions<sup>[12]</sup> and enhance phosphorescence emission.<sup>[13]</sup> In addition, materials that

exhibit RTP can be incorporated into supramolecular composites in which their phosphorescence is enhanced by host–guest interactions. For example, phosphorescent guest molecules can be encapsulated in cyclodextrins to promote phosphorescence emission.<sup>[14,15]</sup> In this study, we took advantage of this phenomenon to develop a strategy<sup>[16]</sup> for increasing the phosphorescence lifetime of an organic phosphor. Specifically the strategy involved noncovalent binding of bromophenyl-methyl-pyridinium chloride (PYCl) to 7-[6-deoxy-6-(2-sulfonic)]- $\beta$ -cyclodextrin (SCD) and a cationic amino clay (AC) to form a hybrid xerogel, designated AC/SCD $\supset$ PYCl, which could be lyophilized to obtain a xerogel with a phosphorescence lifetime 215 times that of free PYCl. This strategy has the following advantages. 1) Host–guest and hydrophobic interactions between SCD and PYCl, as well as electrostatic interactions between the anionic SCD $\supset$ PYCl complexes and the cationic AC, suppressed vibrational and nonradiative relaxation of the phosphor, resulting in phosphorescence emission at 500 nm. 2) The xerogel exhibited good fluorescence–phosphorescence dual emission at room temperature. 3) The hydrogel could be passed through a syringe by applying slight pressure and could be recovered after leaving the needle (**Scheme 1**).

It is well known that incorporating halogen bonding into the crystals of purely organic molecules can result in compounds, such as bromophenylmethyl pyridinium salts, that show efficient phosphorescence emission.<sup>[17]</sup> However, the phosphorescence of such materials is almost undetectable when they are in solution or in an amorphous state. We speculated that immobilization of PYCl might enhance the phosphorescence. For this purpose,

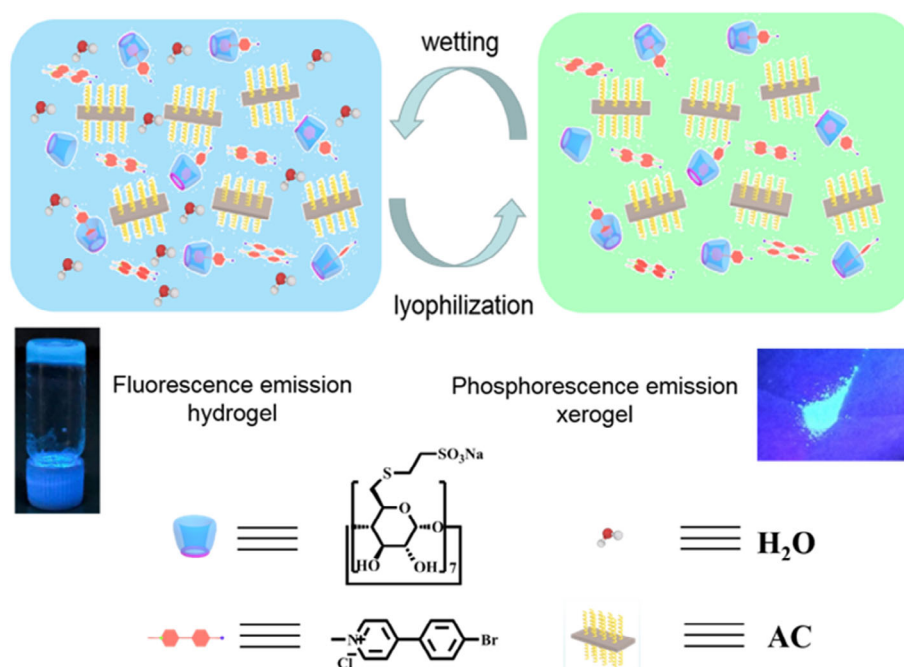
W.-T. Fan, Prof. Y. Chen, Dr. J. Niu, T. Su, Dr. J.-J. Li, Prof. Y. Liu  
State Key Laboratory of Elemento-Organic Chemistry  
College of Chemistry  
Nankai University  
Tianjin 300071, P. R. China  
E-mail: yuliu@nankai.edu.cn

Prof. Y. Chen, Prof. Y. Liu  
Collaborative Innovation Center of Chemical Science and Engineering  
Nankai University  
Tianjin 300071, P. R. China

 The ORCID identification number(s) for the author(s) of this article can be found under <https://doi.org/10.1002/adpr.202000080>.

© 2020 The Authors. Published by Wiley-VCH GmbH. This is an open access article under the terms of the Creative Commons Attribution License, which permits use, distribution and reproduction in any medium, provided the original work is properly cited.

DOI: 10.1002/adpr.202000080



**Scheme 1.** Construction of the AC/SCD-PYCl hybrid hydrogel and xerogel.

we chose a new type of synthetic AC that has various applications<sup>[18]</sup> and can be prepared by means of a one-step reaction at room temperature.<sup>[19]</sup> The amino groups on the AC surface tend to be protonated in polar solvents, which makes the surface positively charged. Therefore, this AC has good dispersibility and is widely used for constructing hydrogels.<sup>[19]</sup>

## 2. Results and Discussion

We began by using  $^1\text{H}$  NMR to investigate the complexation of PYCl with SCD. When equimolar amounts of SCD and PYCl were combined in aqueous solution, the  $^1\text{H}$  NMR signals of the  $\text{H}_\text{c}$ ,  $\text{H}_\text{d}$ , and  $\text{H}_\text{e}$  protons of PYCl were shifted downfield, the  $\text{H}_\text{b}$  proton was shifted upfield, and the  $\text{H}_\text{d}$  and  $\text{H}_\text{e}$  protons split (**Figure 1**); in addition, the signals of all the SCD protons shifted upfield. ROESY (rotating-frame Overhauser effect spectroscopy, **Figure S11**, Supporting Information) showed clear nuclear Overhauser effect correlations between the PYCl protons and the protons inside the SCD cavity. These experimental results demonstrate that PYCl was encapsulated in the SCD cavity and that the pyridinium moiety of PYCl was adjacent to the sulfonate moiety of SCD. The electrostatic interactions between the pyridinium and sulfonate moieties, in combination with hydrophobic interactions between the host and guest molecules, stabilized the SCD-PYCl complex.

Subsequently, we used UV-vis spectroscopy to study the PYCl/SCD binding ratio for the host-guest complex. When the sum of the concentrations of the two components was fixed at 0.1 mM, a Job's curve indicated that the change in absorption intensity ( $\Delta A$ ) was highest when the fraction of the guest molecule ( $X_\text{guest}$ ) was 0.5 (**Figure S12**, Supporting Information), which proves that the binding ratio was 1:1. On the basis of this

1:1 stoichiometry, we determined the binding constant to be  $5.8 \times 10^4 \text{ M}^{-1}$  by means of UV-vis titration (**Figure S13**, Supporting Information). Moreover, the zeta potential of the SCD-PYCl complex was measured to be  $-12.95 \text{ mV}$  (**Figure S5**, Supporting Information), and the zeta potential of the AC was measured as  $+91.1 \text{ mV}$  (**Figure S17**, Supporting Information), indicating that the complex was negatively charged and could thus be expected to associate with the positively charged AC by means of electrostatic interactions to form a hybrid hydrogel.

The AC/SCD-PYCl hybrid hydrogel that formed when the SCD-PYCl complex was mixed with the AC emitted intense blue fluorescence at 380 nm (**Figure 2a**), which was similar to the fluorescence of PYCl in aqueous solution; neither free PYCl nor the SCD-PYCl complex exhibited phosphorescence in aqueous solution. Furthermore, the mechanical properties of hybrid hydrogels were investigated. As shown in **Figure S10b**, Supporting Information, the curves of the storage modulus ( $G'$ ) and loss modulus ( $G''$ ) both increase with the increase of the oscillation strain. Within the oscillation strain range of 0.1–100%,  $G'$  is always larger than  $G''$ , indicating that the supramolecular hydrogel is stable and the physical cross-linking is not damaged. With the oscillating strain further increasing,  $G'$  became less than  $G''$ , indicating a gel-sol transition and the destruction of the hydrogel network. On the basis of these results, we selected a strain of 1% to investigate the relationship between the  $G'/G''$  ratio and the oscillation frequency. As shown in **Figure S10a**, Supporting Information, in the angular frequency range of 0.1–100  $\text{rad s}^{-1}$ ,  $G'$  was always larger than  $G''$ , indicating that the hydrogel had good stability. We also evaluated the injectability of the hydrogel (**Figure S9**, Supporting Information) and found that it could be passed through a syringe

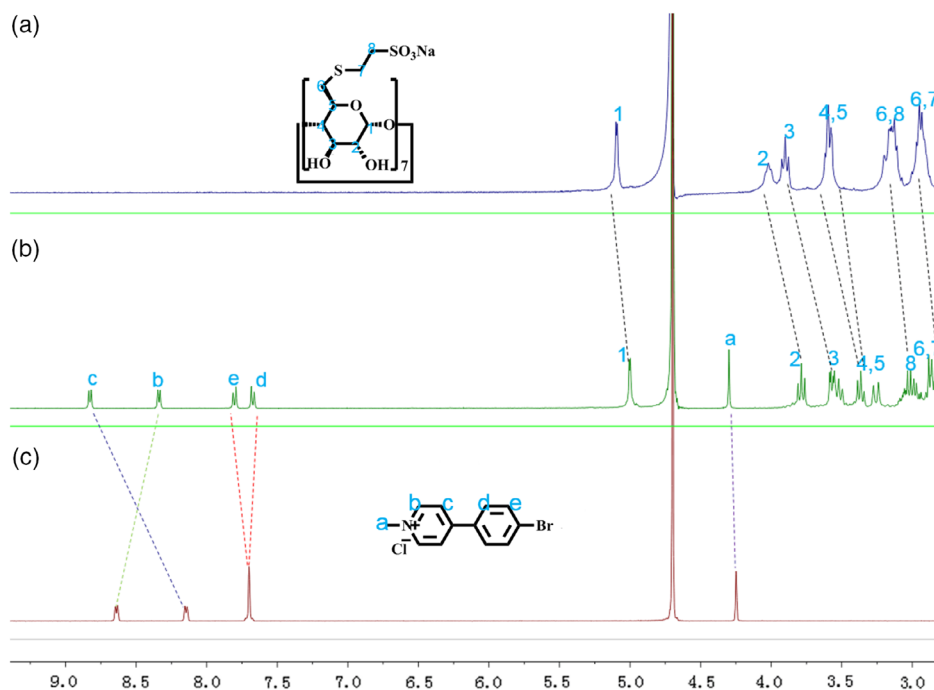


**Figure 1.**  $^1\text{H}$  NMR (400 MHz, 298 K,  $\text{D}_2\text{O}$ ) spectra of a) SCD, b) SCD-PYCl, and c) PYCl ( $[\text{SCD}] = [\text{PYCl}] = 3 \text{ mM}$ ).

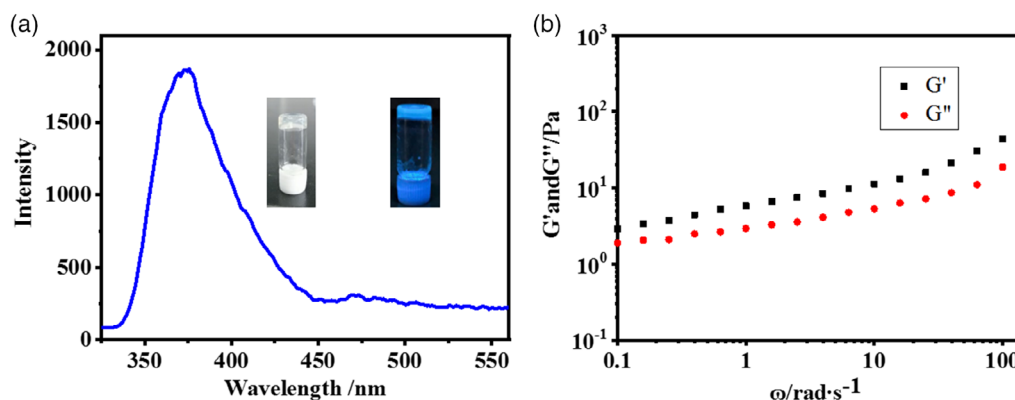


**Figure 2.** a) Fluorescence emission spectrum of the AC/SCD-PYCl hybrid hydrogel at 295 K. Insets: photographs of the hydrogel under natural light (left) and 365 nm light (right). b) Rheological characterization of the hydrogel. Inset: storage modulus ( $G'$ ) and loss modulus ( $G''$ ).

by applying slight pressure, and that the hydrogel will regenerate the gel structure after leaving the needle. This in situ recovery<sup>[20,21]</sup> ability is of great significance for the application of the gel in the field of injectable materials.

Lyophilization of the hydrogel afforded a luminescent xerogel (Figure S8, Supporting Information). Comparison of the photoluminescence spectra of the hydrogel and the xerogel at 295 K (Figure 3a) showed that whereas the hydrogel spectrum had one emission band, the xerogel spectrum had two emission bands, one at 380 nm and the other at 500 nm. The 380 nm band was very similar to the band for aqueous PYCl, indicating that the band should be assigned to fluorescence emission from SCD-PYCl.<sup>[9]</sup> Interestingly, the calculated time-resolved attenuation curve for the band at 500 nm (Figure 3b) showed that it had

a lifetime of 1.24 ms, indicating it to be a phosphorescence emission.

Structural information about the xerogel was obtained by means of scanning electron microscopy and Fourier transform IR spectroscopy (Figure S14 and S15, Supporting Information, respectively). The IR spectrum was very similar to that of the AC, indicating that the AC structure was not altered by formation of the xerogel. The microscopy image showed a clear network structure that can be expected to have restricted vibrational and nonradiative relaxation of the PYCl phosphor.<sup>[22]</sup> Triplet luminescence is generally affected by water, which greatly reduces the intensity of RTP. Therefore, the xerogel showed green fluorescence-phosphorescence dual emission under 365 nm UV irradiation, whereas the hydrogel showed only blue

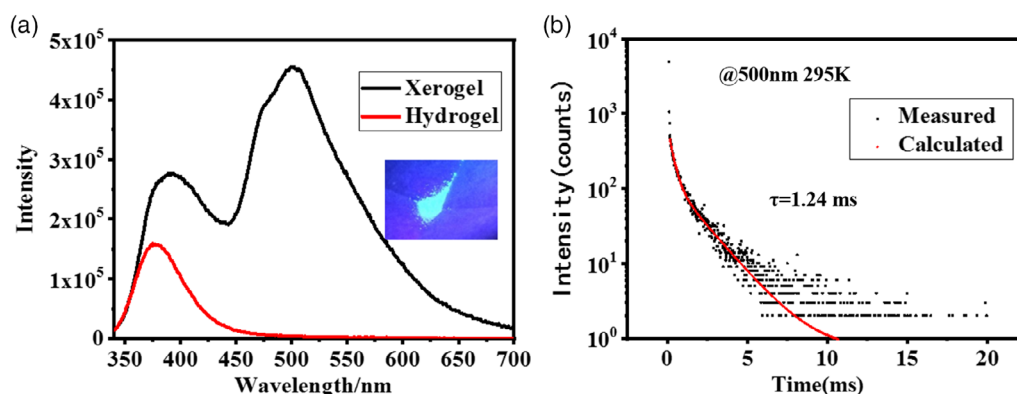


**Figure 3.** a) Photoluminescence spectra of the AC/SCD-PYCl hydrogel (red) and xerogel (black) at 295 K. Inset: photograph of the xerogel under 365 nm UV light. b) Phosphorescence decay curve for the xerogel at 500 nm at 295 K.

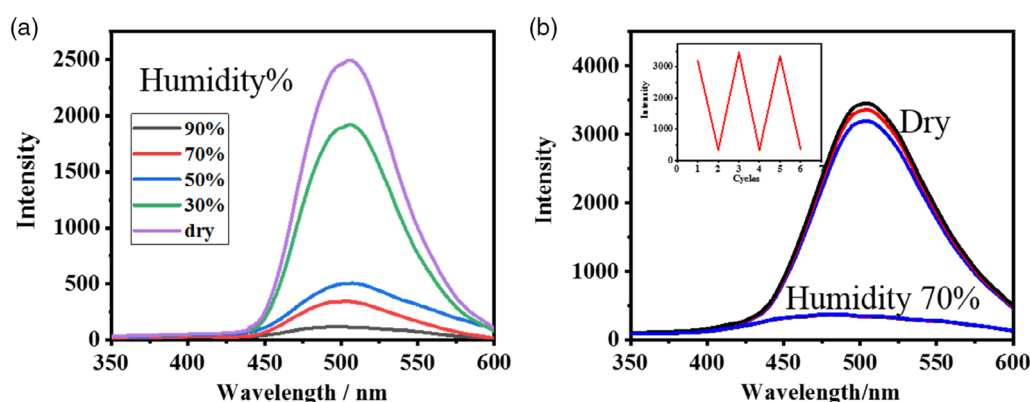


**Figure 4.** a) Effect of humidity on the phosphorescence spectrum of the AC/SCD-PYCl gel and b) phosphorescence spectra (at 503 nm) of the dry gel and the gel at 70% humidity. Inset: variation of the phosphorescence intensity with the number of drying/wetting cycles.

fluorescence under these conditions. On the basis of these findings, we speculated that the water content of AC/SCD-PYCl affected its phosphorescence emission. Therefore, we explored the humidity dependence of the photoluminescence of AC/SCD-PYCl under 365 nm UV irradiation (Figure S16, Supporting Information). These experiments clearly indicated that the photoluminescence intensity varied with humidity (Figure 4a); specifically, the phosphorescence intensity of AC/SCD-PYCl was quenched by 23% to 95% as the humidity was increased from 30% to 90%, respectively. However, the phosphorescence could be almost completely recovered by drying the gel, and this quenching/recovery process could be repeated several times (Figure 4b), suggesting that AC/SCD-PYCl has potential utility as a recyclable humidity sensor. One possible explanation for the reversible phosphorescence of AC/SCD-PYCl may be as follows. As the humidity increases, the AC/SCD-PYCl xerogel absorbs water, which quenches the triplet luminescence, leading to a substantial decrease in the phosphorescence intensity.<sup>[9]</sup> Upon drying of the gel, SCD and the AC jointly provide a restrictive environment for the PYCl molecules, thus increasing their phosphorescence lifetime.<sup>[23]</sup> Next, we changed the concentration of a component in the

xerogel to observe its effect on the dual emission. The results showed that, under the same molar concentration of SCD and PYCl, the phosphorescence emission was enhanced and the fluorescence emission was decreased with the increase of AC concentration. Under the condition of fixed AC concentration, the effect of changing the SCD and PYCl concentration respectively on the dual emission was almost the same (Figure S18, Supporting Information).

### 3. Conclusions

In summary, we prepared a hybrid xerogel composed of PYCl, SCD, and an AC, which are bound together by electrostatic and host-guest interactions. The xerogel has a relatively rigid network structure that effectively fixes the phosphor, limiting vibrational relaxation and thus enhancing RTP. This xerogel has the advantages of being inexpensive, nontoxic, and easy to prepare and process. In addition, it exhibits excellent fluorescence-phosphorescence dual emission at room temperature. In this xerogel, SCD plays a vital role in enhancing the emission behavior of PYCl, and the AC provides a layered environment for the

accumulated PYCl. Due to suppression of vibrational and non-radiative relaxation of the phosphor by the joint effects of the SCD cavity and the gel network structure, this hybrid xerogel can generate a satisfactory RTP signal. In addition, the xerogel responds well to changes in humidity, suggesting its potential utility as an organic light-emitting humidity-sensing material.

## Supporting Information

Supporting Information is available from the Wiley Online Library or from the author.

## Acknowledgements

The authors thank the NSFC (grant nos. 21672113, 21772099, 21971127, and 21861132001) for financial support.

## Conflict of Interest

The authors declare no conflict of interest.

## Keywords

green-light emission, hybrid xerogels, room-temperature phosphorescence, supramolecular assembly

Received: September 25, 2020

Revised: October 11, 2020

Published online:

[1] X. Ma, J. Wang, H. Tian, *Acc. Chem. Res.* **2019**, 52, 738.

[2] J. Zhi, Q. Zhou, H. Shi, Z. An, W. Huang, *Chem. Asian J.* **2020**, 15, 947.

- [3] H. Shi, L. Zou, K. Huang, H. Wang, C. Sun, S. Wang, H. Ma, Y. He, J. Wang, H. Yu, W. Yao, Z. An, Q. Zhao, W. Huang, *ACS Appl. Mater. Interfaces* **2019**, 11, 18103.
- [4] J.-J. Li, H.-Y. Zhang, Y. Zhang, W.-L. Zhou, Y. Liu, *Adv. Opt. Mater.* **2019**, 7, 1900589.
- [5] G. Liu, Y.-M. Zhang, X. Xu, L. Zhang, Y. Liu, *Adv. Opt. Mater.* **2017**, 5, 1700149.
- [6] C. Zhou, H. Li, *New J. Chem.* **2019**, 43, 8439.
- [7] Q. Wang, Z. Zhou, *J. Sol-Gel Sci. Tech.* **2011**, 60, 159.
- [8] Q. Zhang, Y.-X. Deng, H.-X. Luo, C.-Y. Shi, G. M. Geise, B. L. Feringa, H. Tian, D.-H. Qu, *J. Am. Chem. Soc.* **2019**, 141, 12804.
- [9] Z.-Y. Zhang, Y. Chen, Y. Liu, *Angew. Chem., Int. Ed.* **2019**, 58, 6028.
- [10] Z.-Y. Zhang, Y. Liu, *Chem. Sci.* **2019**, 10, 7773.
- [11] S. Cai, H. Shi, J. Li, L. Gu, Y. Ni, Z. Cheng, S. Wang, W.-W. Xiong, L. Li, Z. An, W. Huang, *Adv. Mater.* **2017**, 29, 1701244.
- [12] R. Gao, D. Yan, *Chem. Commun.* **2017**, 53, 5408.
- [13] T. Zhang, X. Ma, H. Wu, L. Zhu, Y. Zhao, H. Tian, *Angew. Chem., Int. Ed.* **2020**, 59, 11206.
- [14] D. Li, F. Lu, J. Wang, W. Hu, X.-M. Cao, X. Ma, H. Tian, *J. Am. Chem. Soc.* **2018**, 140, 1916.
- [15] X.-L. Ni, S. Chen, Y. Yang, Z. Tao, *J. Am. Chem. Soc.* **2016**, 138, 6177.
- [16] Q. Wang, Q. Zhang, Q.-W. Zhang, X. Li, C.-X. Zhao, T.-Y. Xu, D.-H. Qu, H. Tian, *Nat. Commun.* **2020**, 11, 158.
- [17] O. Bolton, K. Lee, H.-J. Kim, K. Y. Lin, J. Kim, *Nat. Chem.* **2011**, 3, 205.
- [18] K. K. R. Datta, A. Achari, M. Eswaramoorthy, *J. Mater. Chem. A* **2013**, 1, 6707.
- [19] a) J. Niu, Y. Chen, Y. Liu, *Soft Matter* **2019**, 15, 3493; b) J. Niu, Y. Chen, Y. Liu, *Chin. J. Org. Chem.* **2019**, 39, 151.
- [20] Y. Deng, Q. Zhang, B. L. Feringa, H. Tian, D.-H. Qu, *Angew. Chem., Int. Ed.* **2020**, 59, 5278.
- [21] Q. Zhao, Y. Chen, Y. Liu, *Chin. Chem. Lett.* **2018**, 29, 84.
- [22] P. Sun, Z. Wang, Y. Bi, D. Sun, T. Zhao, F. Zhao, W. Wang, X. Xin, *ACS Appl. Nano Mater.* **2020**, 3, 2038.
- [23] Y. Deng, P. Li, H. Jiang, X. Ji, H. Li, *J. Mater. Chem. C* **2019**, 7, 13640.